

Control of polariton scattering in resonant-tunneling double-quantum-well semiconductor microcavities

Gabriel Christmann,* Christopher Coulson, and Jeremy J. Baumberg
Cavendish Laboratory, University of Cambridge, Cambridge CB3 0HE, United Kingdom

Nikolaos T. Pelekanos, Zacharias Hatzopoulos, Simeon I. Tsintzos, and Pavlos G. Savvidis
Department of Materials Science and Technology, University of Crete, and FORTH, P.O. Box 1385, 71110 Heraklion, Greece
 (Received 18 July 2010; published 17 September 2010)

Electronic control of ultrafast optical amplification is achieved in specially designed semiconductor microcavities with double quantum well. The gain from parametric scattering of polaritons is selectively quenched by tuning the intracavity electric field to turn on and off interwell resonant tunneling. A $>90\%$ reduction in optical gain is observed with only 100 mV change in applied bias. The strong exciton-photon coupling regime leads here to competition between the rate of Rabi coupling and of electronic tunneling between adjacent quantum wells.

DOI: 10.1103/PhysRevB.82.113308

PACS number(s): 71.36.+c, 42.65.Yj, 73.40.Gk, 78.47.J-

The many unusual phenomena observed when light and electronic excitations are coherently coupled in semiconductor microcavities (SMCs) has revitalized interest in semiconductor quantum electrodynamics over the last ten years. The ability to create strongly coupled systems in which energy oscillates from quantum-confined excitons (in quantum wells or dots) to cavity photons faster than any damping process leads to new polaritonic quasiparticles with radically different nonlinear optical properties than their constituents.¹⁻³ In monolithic planar SMCs, the observation of enormous ultrafast optical amplification of light in 2000 (Refs. 4 and 5) which arises from resonant polariton-polariton scattering fostered, in particular, an extensive research effort culminating more recently in the reports of Bose-Einstein condensation of polaritons,^{6,7} novel parametric processes,^{8,9} and room-temperature polariton lasers.^{10,11}

The first phase of such all-optical exciton-polariton interactions has now moved on to a second phase exploring electrical injection and control in such SMCs. Recent reports of near-room-temperature polariton light-emitting diodes (LEDs) (Refs. 12–15) and bistable properties¹⁶ show how electrical-pumped emission can be enabled but these do not yet control the polariton interactions.

Here we demonstrate a paradigm for manipulating polariton interactions, by incorporating electronic tunneling into p - i - n microcavities. Tunneling of electrons is played off against exciton-light coupling to control the polariton amplification process on picosecond time scales. This resembles operation of quantum cascade intersubband microcavities¹⁷ and lasers¹⁸ but permutes the tunneling and optical processes to give different phenomena. In so doing, we demonstrate a self-limiting electron transfer which “digitally” injects precise charge densities to turn off polariton scattering efficiently ($>90\%$ for $\Delta V=100$ mV applied), and can potentially be used in a variety of ultrahigh-speed modulation schemes.

Electrical control of stimulated scattering is realized in a strongly coupled SMC [Fig. 1(a)] consisting of a $5\lambda/2$ cavity containing four sets of 10 nm $\text{In}_{0.1}\text{Ga}_{0.9}\text{As}$ double quantum wells (DQWs) separated by 20 nm GaAs barriers, placed at the antinodes of the electric field. The cavity is formed from top (17-pair, p -doped) and bottom (21-pair n -doped) GaAs/

AlAs distributed Bragg reflectors (DBRs). A 5.8 meV Rabi splitting is measured at 7.5 K in this structure. Polariton LEDs are processed into 400 μm diameter mesas with a ring-shaped Ti/Pt electrode deposited after a second etch step to contact the lower p layers, improving the series resistance. Similar samples exhibited room temperature polariton emission under electrical injection.¹⁵

Polariton amplification is produced by exciting with 1 ps pump pulses injected at the magic angle ($\sim 16^\circ$) for resonant parametric scattering. In this scheme, two pump polaritons at k_p mutually scatter to yield signal polaritons at $k_s=0$, and idler polaritons at $k_I=2k_p$ [Fig. 1(b), top]. The pump is spectrally filtered to 1.6 meV around the lower polariton energy

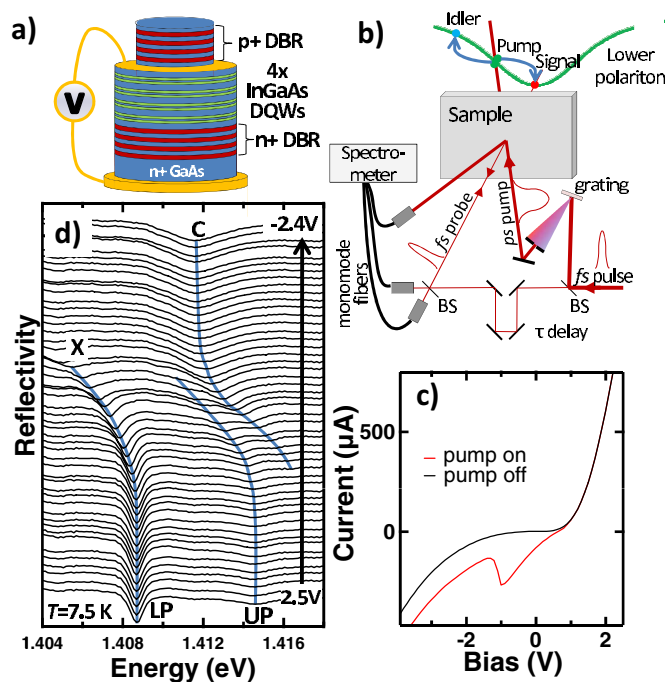


FIG. 1. (Color online) (a) Polariton LED structure. (b) Experimental setup. (c) Current vs applied bias without lasers (black line) and with pump and probe on [red (dark gray) line]. (d) Probe reflectivity spectra for applied biases from 2.5 to -2.4 V, shifted for clarity. Blue (dark gray) lines are guide to eyes.

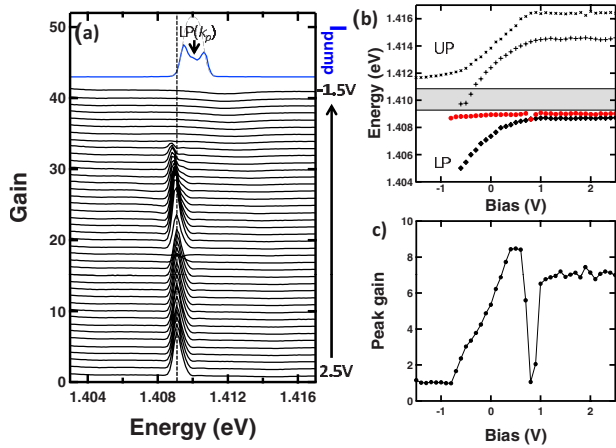


FIG. 2. (Color online) (a) Gain spectra for applied bias from 2.5 to -2.4 V (shifted for clarity), vertical dashed line is a guide to eyes. Reflected pump spectrum also shown [blue (dark gray), top], and gray dashed line is the full pump spectrum. (b) Peak positions for gain [red (dark gray) circles] and polariton branches extracted from reflectivity spectra (+, \times , \blacklozenge). (c) Peak probe gain vs bias.

to avoid exciting higher energy states, and focused to an $80 \mu\text{m}$ spot. This is overlapped with a time-delayed broadband 150 fs probe pulse focused to a $50 \mu\text{m}$ spot at normal incidence. The probe reflectivity from the sample held at $T = 8$ K is collected and directed into both a spectrometer and a balanced photodiode setup which extracts the pump-induced change in probe reflectivity (not shown). External bias applied across the p - i - n allows simultaneous collection of the current. Typical IV scans [Fig. 1(c)] without the pump pulses (black) show a characteristic p - i - n diode response.

The effect of the applied bias is first investigated on the bare polariton modes [Fig. 1(d)]. The normalized probe reflectivity spectra (without pump) clearly show the bias tuning of the polariton modes through the strong-coupling anticrossing. Due to the quantum-confined Stark effect the exciton energy redshifts with increasing electric field while the exciton oscillator strength reduces.¹⁹ The observation of a weak additional anticrossing on the upper polariton is not important for the polariton scattering which is confined to the lower polariton (LP) branch.

Measurements of the probe gain due to parametric scattering are performed for each applied bias, by normalizing the reflected probe spectrum when the pump is on to the incident probe [Fig. 2(a)]. The reflected pump spectrum recorded at zero bias [blue (dark gray)] shown for comparison clearly shows the resonant LP dip at 16° . The gain spectra are recorded at the peak of the amplification at zero delay between pump and probe, and the 3 ps dynamics (not shown but as Ref. 4) is found to be independent of the bias as expected. The spectral positions of polariton modes and gain are extracted [Fig. 2(b)] revealing an almost dispersionless gain peak (red circles).

This dispersionless gain which does not follow the bare LP field tuning indicates that the pump photoinjected carriers eventually tunnel out into the doped DBRs at sufficiently negative applied bias, $V_b < 0.7$ V. The resulting charging of the DBRs reduces the electric field across the i region and

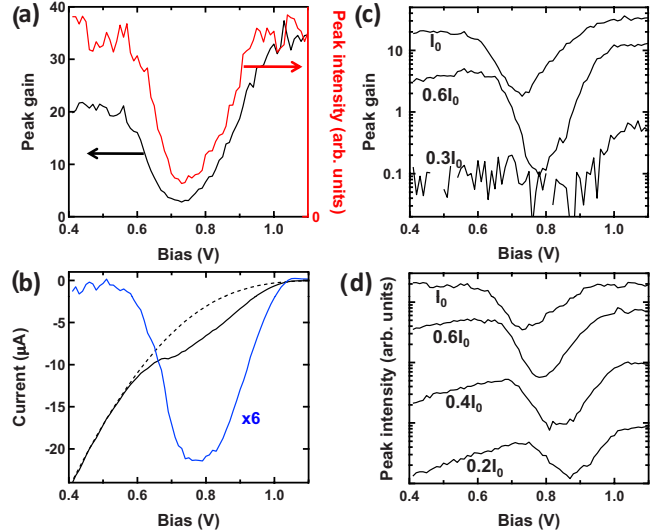


FIG. 3. (Color online) (a) Peak gain vs applied bias (black line) and spontaneous pump-induced stimulated scattering to $k=0$ [red (dark gray) line] from 1.1 to 0.4 V. (b) Photocurrent I vs bias for pump on (black line), with fit I_e calculated for tunneling through triangular barrier (black dashed line) and resulting excess photocurrent (blue line $= I - I_e$). (c) and (d) Pump power dependence of bias-induced dip in (c) polariton gain, and (d) pump-induced spontaneous scattering, $I_0 = 6$ mW.

brings the LP back into resonance, thus maintaining the gain at the original LP energy. This can be clearly tracked in the enhanced tunneling photocurrent [red curve, Fig. 1(c)], with similar field screening as seen previously.¹⁶ Eventually too few carriers are injected to sufficiently screen the applied field, the positive feedback of retuning turns off, and the photocurrent collapses at $V_b = -1$ V.

To explore electrical control of parametric scattering of polaritons, the bias dependence of the peak gain is extracted in Fig. 2(c). At more negative bias, the parametric gain is progressively lost, as the pump overlap with the LP dispersion becomes increasingly difficult to maintain. Interestingly, the gain is *not* reduced at positive bias, despite the simultaneous electrical injection of carriers into the DQWs, and yields clear electroluminescence from the polariton LED while the parametric scattering is occurring. However in addition to this behavior, a dramatic dip in gain is seen around $V_t = 0.7$ V, which is the main focus of this Brief Report. This very strong reduction in gain over a small voltage range (~ 0.1 V) suggests a completely different mechanism to the loss of parametric amplification at negative voltages. Indeed at this voltage, the electric field is so weak that the transition energy is almost unaffected [see Fig. 2(b), \blacklozenge] so the pump is kept in resonance with the lower polariton without the need of electric field screening. Confirming this is the suppressed photocurrent (which only grows exponentially at more negative bias) so that tunneling and corresponding field compensation are negligible at these positive bias (> 0.6 V), contrary to what is observed at negative bias. In the rest of this Brief Report, we focus exclusively on this gain dip and discount the minimal internal field screening.

This sharp gain dip is analyzed in more detail in Fig. 3 which reports the extracted gain and photocurrent. The gain

dip is centered at $V_t=0.73$ V with a reduction of more than 90%. Even if the spectral tuning and spectral bandwidth of the pump are changed, these key characteristics remain unchanged, with only minor modifications of the gain strength either side of the dip. Similar quenching of emission is seen in the spontaneously seeded regime (without the probe beam) [Fig. 3(a), red], which arises from a similar pair scattering mechanism. At the same bias a photocurrent anomaly is observed which corresponds to a local photocurrent peak superimposed on the monotonously increasing background photocurrent, I_e [Fig. 3(b), black line]. The background photocurrent originates from the field-dependent electron tunneling out of the DQWs through the triangular barriers. For a single QW, the tunneling rate, τ_e , is given by²⁰

$$\tau_e = \frac{2m^*L_{\text{QW}}^2}{\hbar\pi} \exp\left\{\frac{4}{3\hbar eF} \sqrt{2m^*U^3}\right\} \approx 180 \text{ ns}$$

for electrons where m^* is the effective mass, L_{QW} the QW thickness, U the confinement potential, and F the electric field. The photocurrent $\propto \tau_e^{-1}$ fits this equation (dashed line), giving an excess photocurrent peak ($\Delta I = I - I_e$, blue line) at 0.77 V associated with the appearance of the gain dip. Varying the pump power [Figs. 3(c) and 3(d)] does not strongly affect the bias position as discussed below. These observations indicate that tunneling of electrons at a very specific electric field is responsible for the gain switching.

To discuss the various processes involved, we consider the band structure in Fig. 4(a), which shows calculated electron and hole ground states. The field tuning of the DQWs [Fig. 4(b)] shows that at an electric field of $V_t = 11.4$ kV cm⁻¹, the electron $n=1$ level of the left QW (LQW) is exactly $\omega_{\text{LO}}=36$ meV above the $n=1$ level of the right QW (RQW). As $F=(V_g-V_b)/L_i$, with built-in potential $V_g=1.52$ V and undoped i thickness $L_i=803$ nm, this corresponds to a bias of 0.61 V in reasonable agreement with the gain dip position. The slightly higher bias than predicted for this resonance is probably due to a voltage drop in the more resistive p -type DBR. We note the $n=1$ LQW to $n=2$ RQW resonance should occur at 15.5 kV cm⁻¹, at $V_b=0.3$ V where carrier escape dominates, obscuring any associated effects. The origin of the bias-controlled gain is thus LO-phonon-assisted resonant tunneling of electrons into the RQW from polaritons in the LQW.^{21,22}

Several key time scales balance the exciton Rabi flopping and electron tunneling [Fig. 4(a)]. The pump pulse excites polaritons in both QWs simultaneously and these oscillate between photon and exciton components every $\tau_\Omega=700$ fs while leaking out of the cavity with a decay time, $\tau_c=8$ ps. The LO-phonon-assisted resonant tunneling is estimated to take $\tau_t=25$ ps, implying that $(1+\tau_t/\tau_c)^{-1} \approx 20\%$ of the electrons from the LQW tunnel into the RQW. This process is followed by an extremely rapid LO-phonon emission, $\tau_{\text{LO}}=100$ fs, considerably faster than the tunneling escape out of the RQW ($\tau_o=230$ fs) implying that 70% of electrons drop into the ground state of the RQW, where they remain for $\tau_e=180$ ns. For the 5 mW pump powers used here this implies that the electron density tunneling to the RQW per pulse is $n_e=1 \times 10^{10}$ cm⁻².

However this omits consideration of the sharp LO-phonon

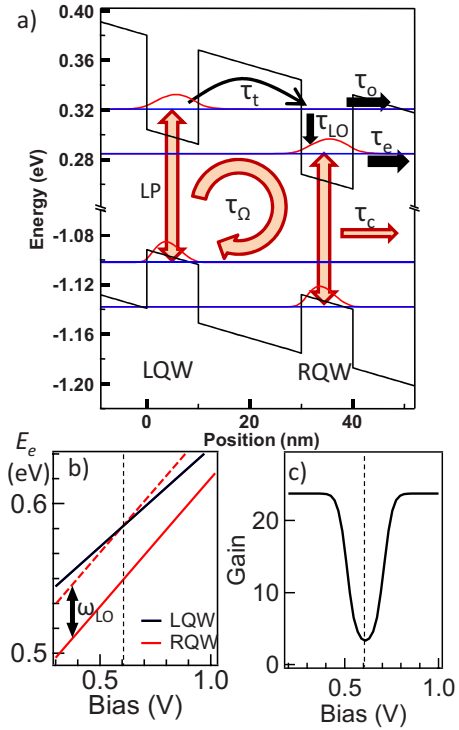


FIG. 4. (Color online) (a) Band edges for the DQW in an electric field, $F=11.4$ kV cm⁻¹. Probability densities for lowest energies shown [red (dark gray) lines], blue/brown arrows show carrier/polariton processes. (b) Energy of lowest electron states in right (RQW) and left (LQW) wells vs field, LO-phonon above RQW ground state shown dashed. (c) Modeling of the gain dip (see text for details).

resonance of measured half width $\Delta V_b=100$ mV corresponding to a potential difference of $\Delta U=4$ meV between the DQWs. The same potential is created for the DQW separation, $d=30$ nm, if a critical electron density, $n_c = \epsilon_r \epsilon_0 \Delta U / ed = 8 \times 10^9$ cm⁻² transfer from the LQW to the RQW. Hence at the resonant bias V_t , enough electrons rapidly tunnel into the RQW to shift the DQW levels back out of the tunneling resonance.

The remaining bound electrons and holes continue to participate in the polariton dynamics, however the resonant tunneling process destroys the gain. Polaritons have been shown to be rather sensitive to interactions with free electrons.^{23,24} In particular, because of their lighter effective mass, electrons are ten times more efficient scatterers than holes.²⁵ The resulting interaction with extra electrons tunneling from the LQW in the RQW creates additional dephasing, thus broadening the polariton modes.²³ As the polaritons cycle through the cavity photon every 700 fs, the signal and idler LPs are delocalized over *both* QWs, thus experiencing the full carrier scattering. Since the coupled signal-idler parametric amplification is strongly dependent on the polariton linewidth,²⁶ this creates the observed dramatic loss of parametric amplification. Combining these microscopic dynamical simulations of the tunneling and the parametric scattering processes²⁷ allows the gain dip to be modeled [Fig. 4(c)]. The carrier-density-dependent broadening of the idler is parametrized from Ref. 23 while the tunnelling linewidth of 4 meV used to

fit the data arises from the 500 fs intersubband decay time found both experimentally and theoretically from LO-phonon emission in 10 nm GaAs QWs.²⁸ This model is in good agreement with the data [Fig. 3(a)] confirming the proposed mechanism.

This saturation of the tunneling injects identical electron densities into the RQW, independent of the laser power (for the regime of stimulated polariton scattering). Indeed we observe the same effect for all pump laser powers for which we can observe the parametric gain process [Figs. 3(c) and 3(d)], with the quenching in fact being proportionally larger at smaller pump powers, consistent with Ref. 26. The gain dip bias is almost independent of pump power, as expected for negligible electric field screening at these positive voltages (electric field compensation should be power dependent). We do not observe any clear bistability for the gain quenching, as also expected from the “digital” electron concentration transferred in a pulsed experiment. If smaller mesa devices down to 1 μm^2 are utilized, the switching energies can be extremely small with only tens of electrons involved in the gain quenching. The speed of the quenching process suggests

that this modulation, which can be both optically or electrically controlled, can approach 1 THz, and thus may be of technological interest. We note that the reset time of the device is controlled by τ_e which is independently set by the heterostructure design.

In conclusion, we have demonstrated an original way to control parametric gain in semiconductor microcavities incorporating double quantum wells. Stark tuning and resonant tunneling between neighboring quantum wells allows dramatic changes in the strong-coupling-induced optical gain for minimal applied bias changes. Given the Stark tuning mechanism involved, ultrafast switching speeds are expected, with similar loss control as in intersubband modulators.²⁹ In addition, we suggest spatial control and quantum entanglement of polaritons in microcavities can be possible using spatially localized electron tunneling.

This work was supported by UK EPSRC under Grants No. EP/C511786/1 and No. EP/F011393 and EU CLERMONT4.

*gprmc2@cam.ac.uk

- ¹C. Ciuti, P. Schwendimann, and A. Quattropani, *Semicond. Sci. Technol.* **18**, S279 (2003), special issue on Microcavities, edited by J. J. Baumberg and L. Viña.
- ²J. P. Reithmaier, G. Şek, A. Löffler, C. Hofmann, S. Kuhn, S. Reitzenstein, L. V. Keldysh, V. D. Kulakovskii, T. L. Reinecke, and A. Forchel, *Nature (London)* **432**, 197 (2004).
- ³T. Yoshie, A. Scherer, J. Hendrickson, G. Khitrova, H. M. Gibbs, G. Rupper, C. Ell, O. B. Shchekin, and D. G. Deppe, *Nature (London)* **432**, 200 (2004).
- ⁴P. G. Savvidis, J. J. Baumberg, R. M. Stevenson, M. S. Skolnick, D. M. Whittaker, and J. S. Roberts, *Phys. Rev. Lett.* **84**, 1547 (2000).
- ⁵R. M. Stevenson, V. N. Astratov, M. S. Skolnick, D. M. Whittaker, M. Emam-Ismael, A. I. Tartakovskii, P. G. Savvidis, J. J. Baumberg, and J. S. Roberts, *Phys. Rev. Lett.* **85**, 3680 (2000).
- ⁶J. Kasprzak, M. Richard, S. Kundermann, A. Baas, P. Jeambrun, J. M. J. Keeling, F. M. Marchetti, M. H. Szymańska, R. André, J. L. Staehli, V. Savona, P. B. Littlewood, B. Deveaud, and Le Si Dang, *Nature (London)* **443**, 409 (2006).
- ⁷R. Balili, V. Hartwell, D. Snoke, L. Pfeiffer, and K. West, *Science* **316**, 1007 (2007).
- ⁸C. Diederichs, J. Tignon, G. Dasbach, C. Ciuti, A. Lemaître, J. Bloch, Ph. Roussignol, and C. Delalande, *Nature (London)* **440**, 904 (2006).
- ⁹C. Leyder, T. C. H. Liew, A. V. Kavokin, I. A. Shelykh, M. Romanelli, J. Ph. Karr, E. Giacobino, and A. Bramati, *Phys. Rev. Lett.* **99**, 196402 (2007).
- ¹⁰S. Christopoulos, G. Baldassarri Höger von Högersthal, A. J. D. Grundy, P. G. Lagoudakis, A. V. Kavokin, J. J. Baumberg, G. Christmann, R. Butté, E. Feltn, J.-F. Carlin, and N. Grandjean, *Phys. Rev. Lett.* **98**, 126405 (2007).
- ¹¹J. J. Baumberg, A. V. Kavokin, S. Christopoulos, A. J. D. Grundy, R. Butté, G. Christmann, D. D. Solnyshkov, G. Malpuech, G. Baldassarri Höger von Högersthal, E. Feltn, J.-F. Carlin, and N. Grandjean, *Phys. Rev. Lett.* **101**, 136409 (2008).
- ¹²S. I. Tsintzos, N. T. Pelekanos, G. Konstantinidis, Z. Hatzopoulos, and P. G. Savvidis, *Nature (London)* **453**, 372 (2008).
- ¹³D. Bajoni, E. Semenova, A. Lemaître, S. Boucoule, E. Wertz, P. Senellart, and J. Bloch, *Phys. Rev. B* **77**, 113303 (2008).
- ¹⁴A. A. Khalifa, A. P. D. Love, D. N. Krizhanovskii, M. S. Skolnick, and J. S. Roberts, *Appl. Phys. Lett.* **92**, 061107 (2008).
- ¹⁵S. I. Tsintzos, P. G. Savvidis, G. Deligeorgis, Z. Hatzopoulos, and N. T. Pelekanos, *Appl. Phys. Lett.* **94**, 071109 (2009).
- ¹⁶D. Bajoni, E. Semenova, A. Lemaître, S. Boucoule, E. Wertz, P. Senellart, S. Barbay, R. Kuszelewicz, and J. Bloch, *Phys. Rev. Lett.* **101**, 266402 (2008).
- ¹⁷D. Dini, R. Köhler, A. Tredicucci, G. Biasiol, and L. Sorba, *Phys. Rev. Lett.* **90**, 116401 (2003).
- ¹⁸J. Faist, F. Capasso, D. L. Sivco, C. Sirtori, A. L. Hutchinson, and A. Y. Cho, *Science* **264**, 553 (1994).
- ¹⁹T. A. Fisher, A. M. Afshar, D. M. Whittaker, M. S. Skolnick, J. S. Roberts, G. Hill, and M. A. Pate, *Phys. Rev. B* **51**, 2600 (1995).
- ²⁰G. Bastard, J. A. Brum, and R. Ferreira, *Solid State Phys.* (Academic press, New York, 1991), Vol. 44, p. 229.
- ²¹D. Y. Oberli, J. Shah, T. C. Damen, J. M. Kuo, J. E. Henry, J. Lary, and S. M. Goodnick, *Appl. Phys. Lett.* **56**, 1239 (1990).
- ²²J. M. Feng, J. H. Park, S. Ozaki, H. Kubo, N. Mori, and C. Hamaguchi, *Semicond. Sci. Technol.* **12**, 1116 (1997).
- ²³P. G. Lagoudakis, M. D. Martin, J. J. Baumberg, A. Qarry, E. Cohen, and L. N. Pfeiffer, *Phys. Rev. Lett.* **90**, 206401 (2003).
- ²⁴M. Perrin, P. Senellart, A. Lemaître, and J. Bloch, *Phys. Rev. B* **72**, 075340 (2005).
- ²⁵G. Malpuech, A. Kavokin, A. Di Carlo, and J. J. Baumberg, *Phys. Rev. B* **65**, 153310 (2002).
- ²⁶C. Ciuti, P. Schwendimann, B. Deveaud, and A. Quattropani, *Phys. Rev. B* **62**, R4825 (2000).
- ²⁷A. V. Kavokin, J. J. Baumberg, G. Malpuech, and F. Laussy, *Microcavities* (Oxford University Press, Oxford, 2007), pp. 263–265.
- ²⁸R. Ferreira and G. Bastard, *Phys. Rev. B* **40**, 1074 (1989).
- ²⁹A. Harwit and J. S. Harris, *Appl. Phys. Lett.* **50**, 685 (1987).